

Constraints on the two-pion contribution to hadronic vacuum polarization

Gilberto Colangelo^a, Martin Hoferichter^a, Peter Stoffer^{b,c}

^aAlbert Einstein Center for Fundamental Physics, Institute for Theoretical Physics, University of Bern, Sidlerstrasse 5, 3012 Bern, Switzerland

^bDepartment of Physics, University of California at San Diego, La Jolla, CA 92093, USA

^cUniversity of Vienna, Faculty of Physics, Boltzmannngasse 5, 1090 Vienna, Austria

Abstract

At low energies hadronic vacuum polarization (HVP) is strongly dominated by two-pion intermediate states, which are responsible for about 70% of the HVP contribution to the anomalous magnetic moment of the muon, a_μ^{HVP} . Lattice-QCD evaluations of the latter indicate that it might be larger than calculated dispersively on the basis of $e^+e^- \rightarrow$ hadrons data, at a level which would contest the long-standing discrepancy with the a_μ measurement. In this Letter we study to which extent this 2π contribution can be modified without, at the same time, producing a conflict elsewhere in low-energy hadron phenomenology. To this end we consider a dispersive representation of the $e^+e^- \rightarrow 2\pi$ process and study the correlations which thereby emerge between a_μ^{HVP} , the hadronic running of the fine-structure constant, the P -wave $\pi\pi$ phase shift, and the charge radius of the pion. Inelastic effects play an important role, despite being constrained by the Eidelman–Łukaszuk bound. We identify scenarios in which a_μ^{HVP} can be altered substantially, driven by changes in the phase shift and/or the inelastic contribution, and illustrate the ensuing changes in the $e^+e^- \rightarrow 2\pi$ cross section. In the combined scenario, which minimizes the effect in the cross section, a uniform shift around 4% is required. At the same time both the analytic continuation into the space-like region and the pion charge radius are affected at a level that could be probed in future lattice-QCD calculations.

1. Introduction

The uncertainty in the Standard Model prediction for the anomalous magnetic moment of the muon [1–28]

$$a_\mu^{\text{SM}} = 116\,591\,810(43) \times 10^{-11} \quad (1)$$

is currently dominated by HVP, whose leading-order contribution as derived from $e^+e^- \rightarrow$ hadrons cross sections reads [1, 6–12]

$$a_\mu^{\text{HVP}}|_{e^+e^-} = 6\,931(40) \times 10^{-11}. \quad (2)$$

The resulting SM prediction (1) differs from experiment [29]

$$a_\mu^{\text{exp}} = 116\,592\,089(63) \times 10^{-11} \quad (3)$$

by 3.7σ . If this discrepancy were all to be blamed on an incorrect evaluation of the HVP contribution, this would have to be as large as $7\,200 \times 10^{-11}$ to reconcile the central values of the SM and experiment. That such a possibility should in fact be seriously considered has become a pressing issue in view of recent lattice-QCD evaluations. The lattice average performed in Ref. [1] (based on Refs. [30–38])

$$a_\mu^{\text{HVP}}|_{\text{lattice average}} = 7\,116(184) \times 10^{-11} \quad (4)$$

is consistent with both the e^+e^- value (2) (within 1σ), but also with the experimental value (3). The more recent calculation of Ref. [39], $a_\mu^{\text{HVP}} = 7\,087(53) \times 10^{-11}$, quotes a slightly smaller central value, but due to the increased precision lies above the e^+e^- value by 2.3σ , while reducing the tension with Eq. (3) to 1.5σ .

For the second-most-important class of hadronic contributions, hadronic light-by-light scattering (HLbL), the phenomenological estimate $a_\mu^{\text{HLbL}} = 92(19) \times 10^{-11}$ [1, 14–26, 40–45] agrees with $a_\mu^{\text{HLbL}} = 82(35) \times 10^{-11}$ from lattice QCD [27] (including the phenomenological estimate for the charm contribution), in such a way that an average of the two has been used in Eq. (1).

This situation has triggered renewed interest in the consequences of large changes to HVP elsewhere, especially for global electroweak fits due to its impact on the hadronic running of the fine-structure constant α [46–49]. These analyses have shown that to avoid a significant tension with electroweak precision data, the changes to the hadronic cross sections need to be concentrated at low energies, at least below 2 GeV, a scenario indeed indicated by Ref. [39].

In previous work [47–49] changes to the hadronic cross sections were considered as a whole, with specific assumptions on the energy dependence. However, if the changes are concentrated in the low-energy region, it is clear that the most relevant absolute effect will occur in the dominant 2π channel, since the required relative changes in the subleading channels would become prohibitively large. In this region, the 2π channel is essentially elastic and dominated by the ρ resonance. The relevant hadronic matrix element, the pion vector form factor (VFF), is strongly constrained by analyticity and unitarity, which imply that below 1 GeV it is essentially determined by the P -wave $\pi\pi$ phase shift [8], which is again constrained by analyticity, unitarity, and crossing symmetry, taking the form of Roy equations [50–53]. The main conclusion of the analysis in Ref. [8] is that the VFF below 1 GeV can be described in terms of a

handful of parameters, which can all be determined by a fit to the $e^+e^- \rightarrow 2\pi$ data. The fact that these data, which have now reached a remarkable level of precision, typically below 1%, can be well described by this highly constrained representation, is a nontrivial test on their quality.

Within this framework it is possible to address the question which changes become possible without violating analyticity and unitarity and without incurring other tensions elsewhere—besides those with the $e^+e^- \rightarrow 2\pi$ cross-section data. To this end, we first of all determine what changes in the parameters of the dispersive representation may generate the desired change in a_μ^{HVP} . With the same set of parameters we then calculate the P -wave $\pi\pi$ phase shifts, the hadronic running of α , as well as the charge radius of the pion, and thereby establish correlations among all these quantities.

Finally, we identify scenarios in which significant changes to HVP remain possible despite these independent constraints on the pion VFF. The comparison of the resulting predictions for the $e^+e^- \rightarrow 2\pi$ cross section to data allows us to quantify by how much the experimental cross sections would need to be changed to accommodate such an increase in a_μ^{HVP} .

2. The pion vector form factor

The HVP contribution to the anomalous magnetic moment of the muon, expressed in terms of the $e^+e^- \rightarrow \text{hadrons}$ cross section, reads [54, 55]

$$a_\mu^{\text{HVP}} = \left(\frac{\alpha m_\mu}{3\pi}\right)^2 \int_{s_{\text{thr}}}^{\infty} ds \frac{\hat{K}(s)}{s^2} R_{\text{had}}(s),$$

$$R_{\text{had}}(s) = \frac{3s}{4\pi\alpha^2} \sigma(e^+e^- \rightarrow \text{hadrons}), \quad (5)$$

with a known kernel function $\hat{K}(s)$. With the pion VFF $F_\pi^V(s)$ defined as the matrix element of the electromagnetic current j_{em}^μ ,

$$\langle \pi^\pm(p') | j_{\text{em}}^\mu(0) | \pi^\pm(p) \rangle = \pm(p' + p)^\mu F_\pi^V((p' - p)^2), \quad (6)$$

the 2π contribution becomes

$$\sigma(e^+e^- \rightarrow \pi^+\pi^-) = \frac{\pi\alpha^2}{3s} \sigma_\pi^3(s) |F_\pi^V(s)|^2, \quad (7)$$

where $\sigma_\pi(s) = \sqrt{1 - 4M_\pi^2/s}$. Similarly, the two-pion contribution to the hadronic running of α , evaluated at M_Z^2 ,

$$\Delta\alpha_{\text{had}}^{(5)}(M_Z^2) = \frac{\alpha M_Z^2}{3\pi} \int_{s_{\text{thr}}}^{\infty} ds \frac{R_{\text{had}}(s)}{s(M_Z^2 - s)}, \quad (8)$$

is determined by $F_\pi^V(s)$. In both cases, the integration threshold becomes $s_{\text{thr}} = 4M_\pi^2$, and radiative corrections to the cross section are implemented in such a way that vacuum polarization is removed, but final-state radiation (FSR) included. Since Eq. (6) defines the matrix element in pure QCD, this implies that FSR corrections need to be included in the final step, see Ref. [8] for

further details. In addition, we consider the correlation with the pion charge radius

$$\langle r_\pi^2 \rangle = 6 \frac{dF_\pi^V(s)}{ds} \Big|_{s=0} = \frac{6}{\pi} \int_{4M_\pi^2}^{\infty} ds \frac{\text{Im} F_\pi^V(s)}{s^2}, \quad (9)$$

which, contrary to a_μ^{HVP} and $\Delta\alpha_{\text{had}}^{(5)}$, is also explicitly sensitive to the phase of $F_\pi^V(s)$.

In the elastic region, where 2π is again the only relevant intermediate state, $F_\pi^V(s)$ is strongly constrained by analyticity and unitarity. If the elastic region extended all the way to infinity, the solution to the unitarity and analyticity constraints would be given by the Omnès factor [56]

$$\Omega_1^1(s) = \exp \left\{ \frac{s}{\pi} \int_{4M_\pi^2}^{\infty} ds' \frac{\delta_1^1(s')}{s'(s' - s)} \right\}, \quad (10)$$

with the P -wave $\pi\pi$ scattering phase shift $\delta_1^1(s)$. This phase shift, in turn, is strongly constrained by $\pi\pi$ Roy equations [50–53], which further limits the permissible changes in $F_\pi^V(s)$, see Refs. [57–64] for representations that exploit this intimate connection between the VFF and $\pi\pi$ scattering. Below 1 GeV inelastic effects are small, but at the level of precision necessary here, have to be taken into account. To do this we multiply the fully elastic Omnès factor (10) by two additional factors, as in Refs. [8, 58, 59]

$$F_\pi^V(s) = \Omega_1^1(s) G_\omega(s) G_{\text{in}}^N(s), \quad (11)$$

where $G_\omega(s)$ accounts for the isospin-violating 3π cut, which is completely dominated by ρ - ω mixing, and the 4π cut is expanded into a conformal polynomial

$$G_{\text{in}}^N(s) = 1 + \sum_{k=1}^N c_k (z^k(s) - z^k(0)), \quad (12)$$

where the conformal variable

$$z(s) = \frac{\sqrt{s_{\text{in}} - s_c} - \sqrt{s_{\text{in}} - s}}{\sqrt{s_{\text{in}} - s_c} + \sqrt{s_{\text{in}} - s}} \quad (13)$$

permits inelastic phases above the $\pi\omega$ threshold $s_{\text{in}} = (M_{\pi^0} + M_\omega)^2$. The parameter s_c is the value of s mapped to the origin, $z(s_c) = 0$, and is varied around -1 GeV^2 . To ensure the correct threshold behavior, the c_k are related by an additional constraint that removes the S -wave singularity.

In total, the dispersive representation from Ref. [8] then involves the following free parameters: first, the solution of the $\pi\pi$ Roy equations is determined once the phase shifts at $s_0 = (0.8 \text{ GeV})^2$ and $s_1 = (1.15 \text{ GeV})^2$ are specified, so that $\delta_1^1(s_0)$ and $\delta_1^1(s_1)$ are free fit parameters. Second, $G_\omega(s)$ depends on the ω pole parameters as well as the overall strength of ρ - ω mixing. Third, there are $N - 1$ free parameters in $G_{\text{in}}^N(s)$ to describe inelastic effects.

The results for the phase shifts from a fit to VFF data are [8]

$$\delta_1^1(s_0) = 110.4(7)^\circ, \quad \delta_1^1(s_1) = 165.7(2.4)^\circ, \quad (14)$$

but for the purpose of this work it is crucial to understand to within which ranges they can be constrained without relying on

$e^+e^- \rightarrow 2\pi$ data (or $\tau \rightarrow \pi\pi\nu_\tau$). In principle, one could even consider indirect constraints that arise, via the Roy equations, from low-energy data in crossed channels, such as $K_{\ell 4}$ data [65–67], but here we simply quote the results from the partial-wave analyses

$$\begin{aligned} \text{Ref. [68]} : \quad & \delta_1^1(0.79 \text{ GeV}) = 97.5(1.5)^\circ \quad [103.9(6)^\circ], \\ & \delta_1^1(0.81 \text{ GeV}) = 112.1(8)^\circ \quad [116.2(7)^\circ], \\ & \delta_1^1(1.15 \text{ GeV}) = 167.7(3.3)^\circ \quad [165.7(2.4)^\circ], \\ \text{Ref. [69]} : \quad & \delta_1^1(0.795 \text{ GeV}) = 105.0(1.5)^\circ \quad [107.2(6)^\circ], \\ & \delta_1^1(0.81 \text{ GeV}) = 114.0(1.4)^\circ \quad [116.2(7)^\circ], \\ & \delta_1^1(1.15 \text{ GeV}) = 164(6)^\circ \quad [165.7(2.4)^\circ], \end{aligned} \quad (15)$$

where our values, extracted from the global fit to $e^+e^- \rightarrow 2\pi$ data, are shown in brackets for comparison.

The parameters in $G_\omega(s)$ do not need to be considered further because either one would have to be changed beyond any plausible range to produce a relevant effect in a_μ^{HVP} . Finally, if several free parameters in the conformal polynomial are introduced, the resulting inelastic phase shift in general leads to unacceptably large violations of Watson’s final-state theorem [70]. A quantitative phenomenological bound can be formulated based on the ratio

$$r = \frac{\sigma^{I=1}(e^+e^- \rightarrow \text{hadrons})}{\sigma(e^+e^- \rightarrow \pi^+\pi^-)} - 1 \quad (16)$$

of non- 2π to 2π hadronic cross sections for isospin $I = 1$, e.g., for the total phase ψ of the VFF [71, 72]

$$\sin^2(\psi - \delta_1^1) \leq \frac{1}{2} \left(1 - \sqrt{1 - r^2}\right). \quad (17)$$

This EŁ bound shows that inelastic effects below the $\pi\omega$ threshold are indeed negligible, and limits the size of the inelastic phase above. In practice, we use the implementation of the EŁ bound from Ref. [8], but note that these details are of limited importance in the present context: once the EŁ bound becomes active, the increase in the χ^2 is rather steep, so that the excluded parameter space is essentially insensitive to the exact implementation of the EŁ bound.

3. Changing HVP

We start from the main results of Ref. [8], where the representation (11) is fit to a combination of the data sets of Refs. [73–85], leading to a two-pion contribution to a_μ^{HVP} below 1 GeV of [8]

$$\begin{aligned} a_\mu^{\pi\pi}|_{\leq 1 \text{ GeV}} &= 495.0(1.5)(2.1) \times 10^{-10} \\ &= 495.0(2.6) \times 10^{-10}, \end{aligned} \quad (18)$$

where the first error is the fit uncertainty (inflated by $\sqrt{\chi^2/\text{dof}}$) and the second error includes all systematic uncertainties of the representation (11). The central configuration uses $N - 1 = 4$

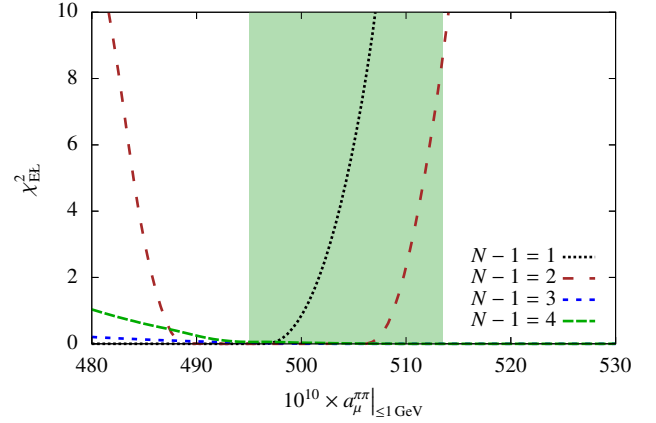


Figure 1: Impact of the EŁ bound on the χ^2 for $N - 1 = 1 \dots 4$ when varying $a_\mu^{\pi\pi}|_{\leq 1 \text{ GeV}}$ away from the central fit result. The shaded area corresponds to $0 \leq \Delta a_\mu^{\pi\pi}|_{\leq 1 \text{ GeV}} \leq 18.5 \times 10^{-10}$ for $N - 1 = 4$.

free parameters in the conformal polynomial. Due to the sensitivity of the radius sum rule (9) to the phase of the VFF, fits with too many free parameters in the conformal polynomial tend to become unstable for $\langle r_\pi^2 \rangle$, because the phase needs to be extrapolated above the energy for which the EŁ bound can be used in practice to constrain the size of the imaginary part. For this reason, in Ref. [8] the central evaluation of $\langle r_\pi^2 \rangle$ was obtained with $N - 1 = 1$, but the full variation with N was kept as a systematic uncertainty, which dominates the uncertainty assigned to the final result [8]

$$\langle r_\pi^2 \rangle = 0.429(1)(4) \text{ fm}^2 = 0.429(4) \text{ fm}^2. \quad (19)$$

Here, we use as reference point the value for $N - 1 = 4$ [8]

$$\langle r_\pi^2 \rangle|_{N-1=4} = 0.426(1) \text{ fm}^2, \quad (20)$$

where the error refers to the fit uncertainty only. Finally, the fit configuration with $N - 1 = 4$ leads to a two-pion contribution to the hadronic running of α , $\Delta\alpha_{\pi\pi}^{(5)}(M_Z^2)$, of

$$\begin{aligned} \Delta\alpha_{\pi\pi}^{(5)}(M_Z^2)|_{\leq 1 \text{ GeV}} &= 32.62(10)(11) \times 10^{-4} \\ &= 32.62(15) \times 10^{-4}. \end{aligned} \quad (21)$$

Starting from the central fit results, we now modify the contribution to a_μ^{HVP} by including in the fit a hypothetical “lattice” observation of $a_\mu^{\pi\pi}|_{\leq 1 \text{ GeV}}$ in the form of an additional contribution to the χ^2 function that we minimize. The fit output for $a_\mu^{\pi\pi}|_{\leq 1 \text{ GeV}}$ is then pulled away from the central fit result in Eq. (18), depending on the input $a_\mu^{\pi\pi}|_{\leq 1 \text{ GeV}}$ and its uncertainty that acts as a weight. We find it convenient to adopt a tiny uncertainty, because it forces the output for $a_\mu^{\pi\pi}|_{\leq 1 \text{ GeV}}$ to essentially coincide with the input. With a larger uncertainty (i.e., a smaller weight) the fit output for $a_\mu^{\pi\pi}|_{\leq 1 \text{ GeV}}$ will be somewhere between the input and Eq. (18). However, the choice of the weights is immaterial because the following studies are all based on the output $a_\mu^{\pi\pi}|_{\leq 1 \text{ GeV}}$. For a given output $a_\mu^{\pi\pi}|_{\leq 1 \text{ GeV}}$, the fit always finds the parameter values that minimize the tension with the cross-section data. We consider the following three scenarios:

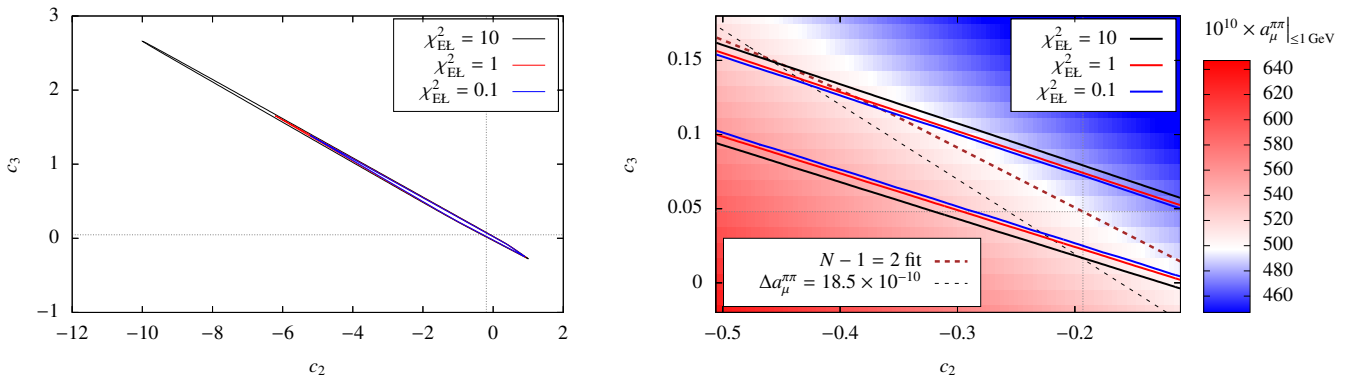


Figure 2: Impact of the EŁ bound on the χ^2 for $N - 1 = 2$ when varying the free parameters c_2 and c_3 away from the central fit result (denoted by dotted lines). Shown are the regions corresponding to $\chi_{\text{EŁ}}^2 \in \{0.1, 1, 10\}$. The right plot shows in more detail the parameter region of interest and the results for $a_{\mu}^{\pi\pi}|_{\leq 1 \text{ GeV}}$ as a heat-map overlay. The brown dashed line shows the path of the fit in scenario (2).

- (1) “Low-energy” scenario: we fix all parameters of the dispersive representation of the VFF to the central fit results with $N - 1 = 4$ without “lattice” input for $a_{\mu}^{\pi\pi}|_{\leq 1 \text{ GeV}}$, apart from the two phase-shift parameters $\delta_1^1(s_0)$ and $\delta_1^1(s_1)$, which are used as free parameters in a fit to data and “lattice” input for $a_{\mu}^{\pi\pi}|_{\leq 1 \text{ GeV}}$.
- (2) “High-energy” scenario: we fix all parameters apart from the parameters c_k in the conformal polynomial.
- (3) Combined scenario: all parameters are used as free fit parameters.

We are interested in the region of the parameter space that allows for a significant upward shift in $a_{\mu}^{\pi\pi}$. For definiteness, we take

$$\Delta a_{\mu}^{\pi\pi}|_{\leq 1 \text{ GeV}} \lesssim 18.5 \times 10^{-10} \quad (22)$$

as reference point, which corresponds to the difference between Eqs. (2) and (4).

The dependence of the VFF on the two free phase parameters $\delta_1^1(s_0)$ and $\delta_1^1(s_1)$ is intertwined with the solution of the Roy equations for the phase $\delta_1^1(s)$, which in turn determines the Omnès function (10). In contrast, the dependence on the parameters in the conformal polynomial is much more direct, as the constraint that removes the S -wave singularity is a linear relation between the parameters c_k . Therefore, the VFF is linear in the parameters c_k and the same is true for the contribution to the charge radius, while $a_{\mu}^{\pi\pi}$ and $\Delta a_{\mu}^{\pi\pi}(M_Z^2)$ are quadratic in the conformal parameters c_k . However, in the relevant parameter range the non-linearities prove to be very small.

In order to further restrict possible variants in scenarios (2) and (3), we first investigate the role of the EŁ bound in the context of variations of $a_{\mu}^{\pi\pi}|_{\leq 1 \text{ GeV}}$.

4. Constraints due to the EŁ bound

The EŁ bound (17) provides an additional restriction on the permissible parameter space that is independent of the two-pion cross-section measurements. Using the implementation

of Ref. [8] and the data compilation of Ref. [72], this constraint leads to a steep rise of the χ^2 function unless the inelastic phase stays small. To illustrate this effect, we consider scenario (2) and fit configurations with $N - 1 = 1 \dots 4$ free parameters in the conformal polynomial. Starting from the central fit results, we vary the input value for $a_{\mu}^{\pi\pi}|_{\leq 1 \text{ GeV}}$. The impact of the EŁ bound on the χ^2 is shown in Fig. 1, as a function of the fit output $a_{\mu}^{\pi\pi}|_{\leq 1 \text{ GeV}}$. We find that the bound severely restricts the possible changes in $a_{\mu}^{\pi\pi}$ for $N - 1 = 1$: inducing larger shifts with only a single free parameter in the conformal polynomial automatically leads to a significant effect in the inelastic phase that violates the EŁ bound, thus excluding such a scenario. With two free parameters in the conformal polynomial, the EŁ bound permits larger changes in $a_{\mu}^{\pi\pi}$, but still imposes a restriction. To evade the EŁ bound for large changes in $a_{\mu}^{\pi\pi}$, more freedom in the parameterization is required, and indeed the situation changes if we consider three or more free parameters in the conformal polynomial, see Fig. 1.

In order to better understand this effect, we consider in some detail the case of $N - 1 = 2$. The fit to data alone leads to

$$a_{\mu}^{\pi\pi}|_{\leq 1 \text{ GeV}}^{N-1=2} = 497.0(1.4) \times 10^{-10}. \quad (23)$$

Varying the two parameters $c_{2,3}$ away from the central fit results, we find that the EŁ bound gives a contribution to the χ^2 that results in a strong anti-correlation between permissible values for the two free parameters. This is illustrated in Fig. 2, where we show the contours for $\chi_{\text{EŁ}}^2 \in \{0.1, 1, 10\}$ in the c_2 - c_3 plane. In the close-up plot, we also overlay a heat map for the resulting value of $a_{\mu}^{\pi\pi}|_{\leq 1 \text{ GeV}}$. Accordingly, for two free parameters in the conformal polynomial the EŁ bound alone no longer excludes very large shifts in $a_{\mu}^{\pi\pi}$, as shown by the ellipses in Fig. 2. However, large parts of the $\chi_{\text{EŁ}}^2$ ellipsis are in strong tension with the cross-section data. Minimizing the total χ^2 in scenario (2) results in the brown dashed path in Fig. 2, which corresponds to the brown curve shown in Fig. 1. For even more free parameters $N - 1 > 2$, the situation remains qualitatively similar: the EŁ bound again strongly correlates the free parameters of the conformal polynomial, essentially imposing

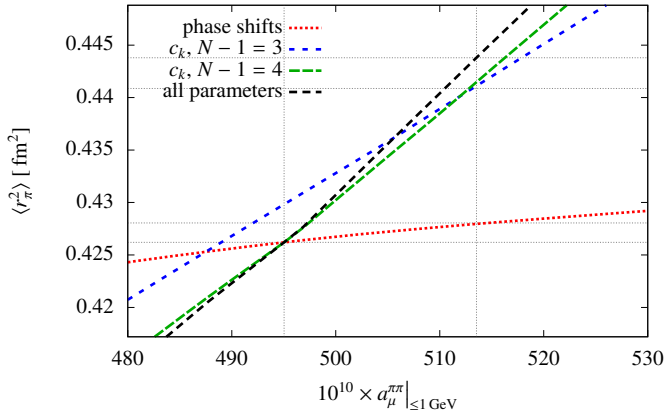


Figure 3: Correlations between $a_\mu^{\pi\pi}$ and $\langle r_\pi^2 \rangle$ as induced in three different scenarios: a “low-energy” scenario (1), where shifts in $a_\mu^{\pi\pi}$ are induced by changes in the phase-shift parameters $\delta_1^1(s_0)$, $\delta_1^1(s_1)$; two “high-energy” scenarios (2), where the shifts are due to changes in the conformal polynomial with $N-1=3$ or $N-1=4$; and a combined scenario (3) with $N-1=4$, where all free parameters in the dispersive representation of the pion VFF are allowed to vary.

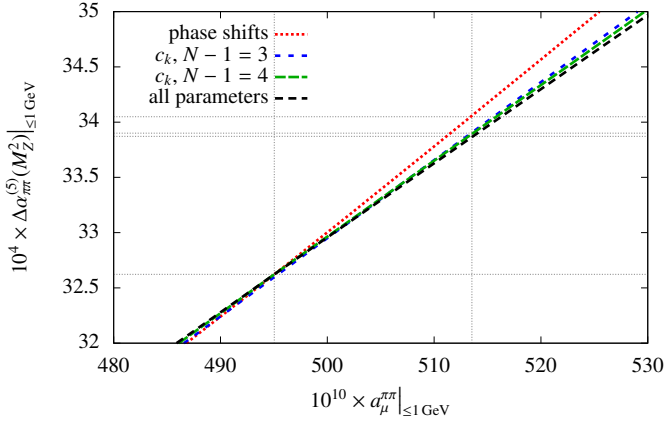


Figure 4: Correlations between $a_\mu^{\pi\pi}$ and $\Delta\alpha_{\pi\pi}^{(5)}(M_Z^2)$ for the same scenarios as in Fig. 3.

one linear constraint, but the values of $a_\mu^{\pi\pi}$ that can be reached are no longer bounded. Therefore, in the following we will only consider fit variants with $N-1=3$ and $N-1=4$, where the EŁ bound is easily fulfilled even for large shifts in $a_\mu^{\pi\pi}$.

5. Correlations with $\Delta\alpha_{\text{had}}^{(5)}$ and $\langle r_\pi^2 \rangle$

We now turn our attention to the correlations among the three quantities derived from HVP—the two-pion contribution to the anomalous magnetic moment of the muon $a_\mu^{\pi\pi}$, the pion charge radius $\langle r_\pi^2 \rangle$, and the two-pion contribution to the hadronic running of α , $\Delta\alpha_{\pi\pi}^{(5)}(M_Z^2)$. We vary the hypothetical “lattice” input for $a_\mu^{\pi\pi}|_{|s| \le 1 \text{ GeV}}$, perform the fits according to the three scenarios defined in Sect. 3, and compute the resulting output values for the three quantities. The results in Figs. 3 and 4 show the correlations of $a_\mu^{\pi\pi}$ with $\langle r_\pi^2 \rangle$ and $\Delta\alpha_{\pi\pi}^{(5)}(M_Z^2)$, respectively, as induced in each of the scenarios.

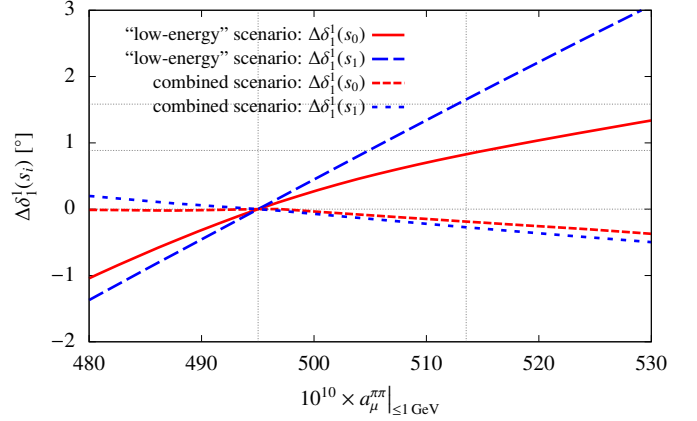


Figure 5: Change in the phase shift δ_1^1 at $s_0 = (0.8 \text{ GeV})^2$ and $s_1 = (1.15 \text{ GeV})^2$ as a function of $a_\mu^{\pi\pi}$. In scenario (1) only these two parameters are used to achieve the change in $a_\mu^{\pi\pi}$, while in the combined scenario (3) all parameters are changed simultaneously.

If the changes in $a_\mu^{\pi\pi}|_{|s| \le 1 \text{ GeV}}$ are induced only by variations of the two phase-shift parameters $\delta_1^1(s_0)$ and $\delta_1^1(s_1)$, they have only little impact on the charge radius $\langle r_\pi^2 \rangle$, see Fig. 3. Hence, in practice changes of $a_\mu^{\pi\pi}$ induced by these parameters cannot be detected by a precision measurement of $\langle r_\pi^2 \rangle$. However, a scenario where the changes in $a_\mu^{\pi\pi}|_{|s| \le 1 \text{ GeV}}$ are induced by shifts in the parameters c_k of the conformal polynomial generates large shifts in $\langle r_\pi^2 \rangle$ and could be constrained by additional information on the charge radius of the pion, at least in principle. At present, lattice determinations of the charge radius [86, 87] have not yet reached the precision that could exclude these shifts: the current lattice uncertainties cover the entire plot range in Fig. 3, but future progress on the determination of the charge radius could further constrain the allowed parameter range. Interestingly, the combined scenario (3) where all parameters are allowed to vary leads to the largest effect in the pion charge radius, even slightly larger than the effect in the scenarios (2). By definition, this is the scenario with minimal tension with the cross-section data, but Fig. 3 shows that this comes at the expense of the largest shift in the charge radius.

In contrast to the pion charge radius, all scenarios lead to very similar correlations with the hadronic running of α , as shown in Fig. 4. A shift in $a_\mu^{\pi\pi}|_{|s| \le 1 \text{ GeV}}$ by 18.5×10^{-10} corresponds to a shift in $\Delta\alpha_{\pi\pi}^{(5)}(M_Z^2)|_{|s| \le 1 \text{ GeV}}$ between 1.2×10^{-4} and 1.4×10^{-4} , as shown in Fig. 4.¹ The existence of such a correlation emerges because we do not allow for arbitrary changes in the hadronic cross section: while in general the two quantities need not be correlated due to the different energy dependence of their kernel

¹This shift is slightly smaller than the 1.8×10^{-4} estimated in Ref. [47] if the relative changes occur below 1.94 GeV but are otherwise energy independent. Shifts of this size violate the bound on $\Delta\alpha_{\text{had}}^{(5)}(M_Z^2)$ derived in Ref. [88]. Since this bound was derived on the basis of assumptions (dim-6 operator as sole origin of the shift in $\Delta\alpha_{\text{had}}^{(5)}(M_Z^2)$ and an arbitrary scale choice when converting the derivative of the HVP function to $\Delta\alpha_{\text{had}}^{(5)}(M_Z^2)$), we have to conclude that these assumptions are not tenable. The result for $\Delta\alpha_{\text{had}}^{(5)}(M_Z^2)$ indicated by Ref. [39] leads to the same conclusion.

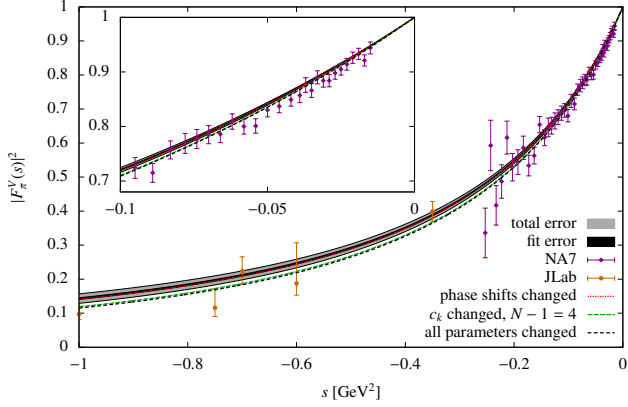


Figure 6: Close-up view of the spacelike region. The JLab data [89–92] are not used in the fit.

functions, we find that a correlation does arise if only changes in the $\pi\pi$ channel are considered as allowed by analyticity and unitarity constraints, while trying to minimize the tension with the $\pi\pi$ cross-section data.

6. Impact on the phase shift and cross section

In scenario (1) we only allow the two phase-shift parameters $\delta_1^1(s_0)$ and $\delta_1^1(s_1)$ to deviate from the central fit results to data. If only the phase at $s_0 = (0.8 \text{ GeV})^2$ were varied, a huge change in the phase shift of about $\Delta\delta_1^1(s_0) = 10^\circ$ would be necessary to obtain a shift in $a_\mu^{\pi\pi}|_{\leq 1 \text{ GeV}}$ by 18.5×10^{-10} . On the other hand, such a change in $a_\mu^{\pi\pi}$ could be induced by the parameter $\delta_1^1(s_1)$ alone with a shift by 1.8° . If we fit the two parameters simultaneously to a combination of the space- and time-like data on the VFF and the hypothetical “lattice” input on $a_\mu^{\pi\pi}|_{\leq 1 \text{ GeV}}$, a shift in $a_\mu^{\pi\pi}|_{\leq 1 \text{ GeV}}$ by 18.5×10^{-10} then corresponds to modest changes in the phase by $\Delta\delta_1^1(s_0) = 0.8^\circ$ and $\Delta\delta_1^1(s_1) = 1.7^\circ$, see Fig. 5. We note that the partial-wave solutions given in Eq. (15) would actually favor values slightly below our reference point (14), but certainly exclude the required change in $\delta_1^1(s_0)$ if the shift in $a_\mu^{\pi\pi}|_{\leq 1 \text{ GeV}}$ were induced by this parameter alone.

As discussed in Sect. 5, indirect constraints on scenario (1) from a determination of the pion charge radius seem out of reach. However, direct constraints on $\delta_1^1(s_0)$ and $\delta_1^1(s_1)$ could be obtained from lattice determinations of the elastic $\pi\pi$ phase shift [93–102], not only at these exact points in energy, but in the whole ρ resonance region: given the phase values $\delta_1^1(s_{0,1})$, the Roy solutions determine the modified phase shift over the whole energy range. However, the precision of lattice data is not yet sufficient to add meaningful constraints to the parameter space, and only a significant increase in precision will have an impact on a_μ^{HVP} determinations.

Figure 5 also shows the resulting shifts in the phase parameters for scenario (3), $\Delta\delta_1^1(s_0) = -0.2^\circ$ and $\Delta\delta_1^1(s_1) = -0.3^\circ$. As discussed in Sect. 5, it is most promising to indirectly constrain such a scenario with an improved determination of the pion charge radius. In fact, not only the radius is relevant in this regard, but the VFF in the whole space-like region, as shown in

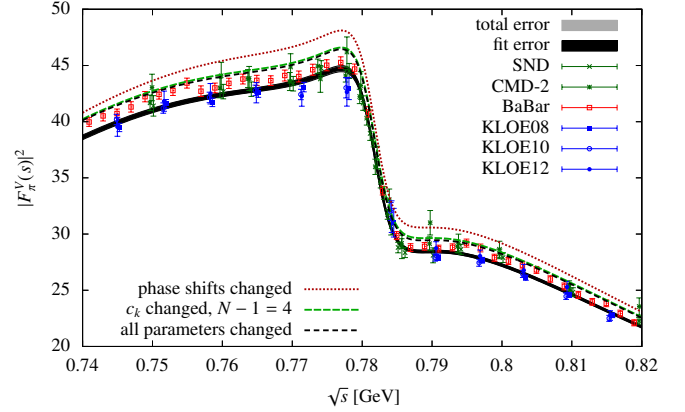


Figure 7: Close-up view of the ρ - ω interference region.

Fig. 6. Scenarios (2) and (3) move the curve outside the error band of the central fit to data. Precise lattice-QCD determinations of the space-like VFF [87] could start to discriminate between the central solution and these shifted variants. Consistently with the small effect on the radius, scenario (1) with shifts only in the two phase-shift parameters has a negligible effect on the space-like VFF: the shifted solution remains well within the uncertainties of the central fit result.

Finally, we take a closer look at the pion VFF in the time-like region. The dispersive representation of the VFF allows us to quantify in detail how the cross sections would need to be altered to achieve a given change in $a_\mu^{\pi\pi}|_{\leq 1 \text{ GeV}}$, in each of the three scenarios. In Fig. 7, a close-up view of the ρ - ω interference region is shown. It reveals that if the change in $a_\mu^{\pi\pi}|_{\leq 1 \text{ GeV}}$ were explained with the help of $\delta_1^1(s_{0,1})$, a dramatic shift of up to 8% of the cross section would be necessary. If the shift were obtained by changing the parameters c_k , the effect in the cross section at the ρ resonance would be only about half as large, although the resulting cross section would still lie far outside the combined fit to the data. The combined scenario is very close to the one where shifts are only allowed in the parameters c_k .

In Fig. 8, we compare both the data sets and the shifted variants of the VFF to the central fit result, as the relative differences normalized to the fit result. We again see that by using the conformal polynomial to induce the shift, the effect on the cross sections is smaller around the ρ resonance than in the scenario with a shift in $\delta_1^1(s_{0,1})$, while the effect is larger below about 0.72 GeV. Compared to the spread of the data points, the necessary shift in the cross sections is again significant, although less drastic than in scenario (1), where the changes are concentrated in the ρ region. This is consistent with the fact that the conformal polynomial parameterizes the effects of inelasticities above the $\pi\omega$ threshold.

While Figs. 7 and 8 make it evident that the changes in the cross section that would generate the desired change in $a_\mu^{\pi\pi}|_{\leq 1 \text{ GeV}}$ are incompatible with the data, Fig. 9 shows the corresponding change in χ^2 as a function of $a_\mu^{\pi\pi}|_{\leq 1 \text{ GeV}}$, and provides a quantitative measure of the discrepancy. The most dramatic clash with the data would be in scenario (1), but even in

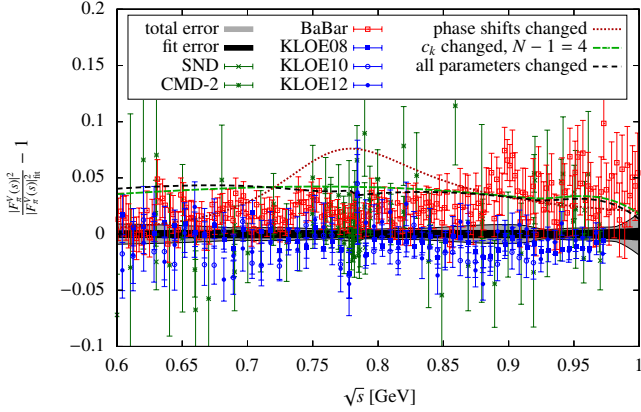


Figure 8: Comparison of the data sets and the shifted variants of the VFF, relative to the central fit solution.

the other two any significant change in $a_{\mu}^{\pi\pi}|_{\leq 1 \text{ GeV}}$ comes at the price of huge increases in χ^2 . These increases can be compared to the well-known tension between individual e^+e^- data sets. The central fit results of Ref. [8] reach a total χ^2 of 776 with 627 degrees of freedom. The tension is reflected by an error inflation included in Eq. (18) of $\sqrt{\chi^2/\text{dof}} = 1.11$. For the target shift of $\Delta a_{\mu}^{\pi\pi}|_{\leq 1 \text{ GeV}} = 18.5 \times 10^{-10}$, even scenario (3) leads to a total χ^2 of 941.

The results in Figs. 7 and 8 show that to minimize the effect in the cross section, the changes mainly affect the inelastic part of the VFF parameterization and thus energies above the $\pi\omega$ threshold. In principle, these inelastic contributions could be further constrained by $e^+e^- \rightarrow 2\pi$ data above 1 GeV [81, 83, 103], $\tau \rightarrow \pi\pi\nu_{\tau}$ [104], and explicit input on the inelastic channels, but this requires an extension of our dispersive formalism that will be left for future work. We remark that any changes in the physics above 1 GeV will also have an impact on $\Delta a_{\pi\pi}^{(5)}(M_Z^2)$, which is not yet accounted for here: the higher in energy these changes are pushed, the higher the risk to exacerbate tensions in the global electroweak fit [46–49].

7. Conclusions

In this Letter we examined the two-pion contribution to HVP in view of recent hints from lattice-QCD calculations that its contribution to the anomalous magnetic moment of the muon could be much larger than obtained from $e^+e^- \rightarrow \text{hadrons}$ cross-section data, with most of the changes concentrated at low energies. We relied on a dispersive representation of the pion vector form factor and studied which of its parameters could be varied without contradicting other low-energy observables besides the $e^+e^- \rightarrow 2\pi$ cross section itself. We identified three scenarios: (1) where only the elastic $\pi\pi$ phase shift, or (2) where only inelastic effects, or (3) all parameters at the same time are allowed to change, see Sect. 3 for more details. In these scenarios, we then derived the correlations with the pion charge radius and the hadronic running of the fine-structure constant.

We found that in scenario (1) the changes in the cross section are mainly concentrated around the ρ resonance, amounting to a

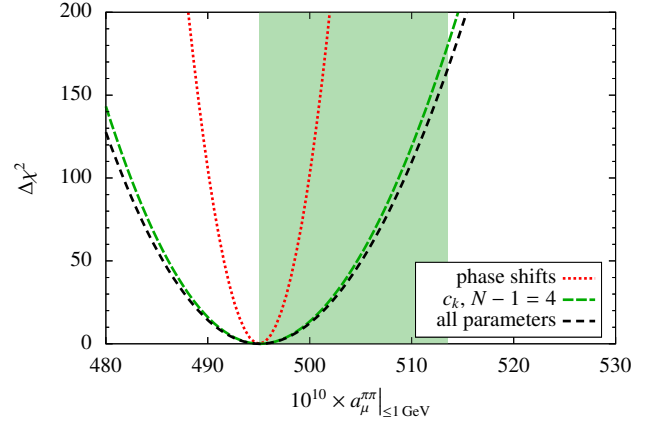


Figure 9: Increase in the χ^2 as a function of the fit output $a_{\mu}^{\pi\pi}|_{\leq 1 \text{ GeV}}$ in the three scenarios, excluding the contribution of the “lattice” input (since this depends on the arbitrary uncertainty that acts as a weight, see Sect. 3).

relative effect of up to 8%, see Figs. 7 and 8, while in scenarios (2) and (3) the changes are more uniformly distributed over the entire energy range, at a level around 4%. The first insight from our analysis is thus that a largely uniform change in the cross section is actually allowed by the constraints from analyticity, unitarity, as well as low-energy hadron phenomenology. Moreover, this is the configuration that minimizes the discrepancy with the data as one tries to increase $a_{\mu}^{\pi\pi}|_{\leq 1 \text{ GeV}}$ while respecting all constraints, but still even this scenario is in strong disagreement with the $e^+e^- \rightarrow 2\pi$ data, see Fig. 9.

The correlations with the pion charge radius and the hadronic running of the fine-structure constant are shown in Figs. 3 and 4, respectively. One of our main conclusions is that in our framework we can establish a firm correlation between $a_{\mu}^{\pi\pi}|_{\leq 1 \text{ GeV}}$ and $\Delta a_{\pi\pi}^{(5)}(M_Z^2)$: the required change in the former implies an upward shift between 1.2×10^{-4} and 1.4×10^{-4} in the latter for all scenarios. For the charge radius the correlation with $a_{\mu}^{\pi\pi}|_{\leq 1 \text{ GeV}}$ depends on the scenario, with the largest effect arising in scenario (3), the one for which the change in the cross section is minimized. A similar observation applies to the entire space-like region, see Fig. 6. This opens the possibility to challenge this scenario with future lattice-QCD calculations of the pion charge radius as well as the space-like pion form factor [86, 87]. Competitive constraints would require a precision around $\Delta \langle r_{\pi}^2 \rangle = 0.005 \text{ fm}^2$, a factor 3 below the sensitivity of Ref. [87]. Similarly, a precision calculation of the P -wave $\pi\pi$ phase shift would provide further independent constraints on our dispersive representation, but here the precision goal of $\Delta \delta_1^1(s_{0,1}) = 2^\circ$ would require significant advances over current calculations.

To further improve the phenomenological determination of the two-pion contribution to HVP, the most important future development naturally concerns new $e^+e^- \rightarrow 2\pi$ data, with BESIII [105, 106] and SND [107] supporting the results already included in the present analysis, and new data from CMD-3 [108] forthcoming. As for direct lattice-QCD evaluations of the HVP contribution, the results of Ref. [39] are being scrutinized by other lattice collaborations, and more detailed

comparisons to phenomenology will allow for refined conclusions as to where the $e^+e^- \rightarrow$ hadrons cross section would need to be modified. In addition, a direct measurement of HVP in the space-like region would become possible with the MUonE project [109, 110], providing further complementary information on the role of HVP in the SM prediction for the anomalous magnetic moment of the muon.

Acknowledgments

Financial support by the DOE (Grant No. DE-SC0009919) and the Swiss National Science Foundation (Project No. PCEFP2_181117 and Grant No. 200020_175791) is gratefully acknowledged.

References

- [1] T. Aoyama *et al.*, Phys. Rept. **887**, 1 (2020), arXiv:2006.04822 [hep-ph].
- [2] T. Aoyama, M. Hayakawa, T. Kinoshita, and M. Nio, Phys. Rev. Lett. **109**, 111808 (2012), arXiv:1205.5370 [hep-ph].
- [3] T. Aoyama, T. Kinoshita, and M. Nio, Atoms **7**, 28 (2019).
- [4] A. Czarnecki, W. J. Marciano, and A. Vainshtein, Phys. Rev. **D67**, 073006 (2003), [Erratum: Phys. Rev. **D73**, 119901 (2006)], arXiv:hep-ph/0212229 [hep-ph].
- [5] C. Gnendiger, D. Stöckinger, and H. Stöckinger-Kim, Phys. Rev. **D88**, 053005 (2013), arXiv:1306.5546 [hep-ph].
- [6] M. Davier, A. Hoecker, B. Malaescu, and Z. Zhang, Eur. Phys. J. **C77**, 827 (2017), arXiv:1706.09436 [hep-ph].
- [7] A. Keshavarzi, D. Nomura, and T. Teubner, Phys. Rev. **D97**, 114025 (2018), arXiv:1802.02995 [hep-ph].
- [8] G. Colangelo, M. Hoferichter, and P. Stoffer, JHEP **02**, 006 (2019), arXiv:1810.00007 [hep-ph].
- [9] M. Hoferichter, B.-L. Hoid, and B. Kubis, JHEP **08**, 137 (2019), arXiv:1907.01556 [hep-ph].
- [10] M. Davier, A. Hoecker, B. Malaescu, and Z. Zhang, Eur. Phys. J. **C80**, 241 (2020), [Erratum: Eur. Phys. J. **C80**, 410 (2020)], arXiv:1908.00921 [hep-ph].
- [11] A. Keshavarzi, D. Nomura, and T. Teubner, Phys. Rev. **D101**, 014029 (2020), arXiv:1911.00367 [hep-ph].
- [12] B.-L. Hoid, M. Hoferichter, and B. Kubis, Eur. Phys. J. **C 80**, 988 (2020), arXiv:2007.12696 [hep-ph].
- [13] A. Kurz, T. Liu, P. Marquard, and M. Steinhauser, Phys. Lett. **B734**, 144 (2014), arXiv:1403.6400 [hep-ph].
- [14] K. Melnikov and A. Vainshtein, Phys. Rev. **D70**, 113006 (2004), arXiv:hep-ph/0312226 [hep-ph].
- [15] G. Colangelo, M. Hoferichter, M. Procura, and P. Stoffer, JHEP **09**, 091 (2014), arXiv:1402.7081 [hep-ph].
- [16] G. Colangelo, M. Hoferichter, B. Kubis, M. Procura, and P. Stoffer, Phys. Lett. **B738**, 6 (2014), arXiv:1408.2517 [hep-ph].
- [17] G. Colangelo, M. Hoferichter, M. Procura, and P. Stoffer, JHEP **09**, 074 (2015), arXiv:1506.01386 [hep-ph].
- [18] P. Masjuan and P. Sánchez-Puertas, Phys. Rev. **D95**, 054026 (2017), arXiv:1701.05829 [hep-ph].
- [19] G. Colangelo, M. Hoferichter, M. Procura, and P. Stoffer, Phys. Rev. Lett. **118**, 232001 (2017), arXiv:1701.06554 [hep-ph].
- [20] G. Colangelo, M. Hoferichter, M. Procura, and P. Stoffer, JHEP **04**, 161 (2017), arXiv:1702.07347 [hep-ph].
- [21] M. Hoferichter, B.-L. Hoid, B. Kubis, S. Leupold, and S. P. Schneider, Phys. Rev. Lett. **121**, 112002 (2018), arXiv:1805.01471 [hep-ph].
- [22] M. Hoferichter, B.-L. Hoid, B. Kubis, S. Leupold, and S. P. Schneider, JHEP **10**, 141 (2018), arXiv:1808.04823 [hep-ph].
- [23] A. Gérardin, H. B. Meyer, and A. Nyffeler, Phys. Rev. **D100**, 034520 (2019), arXiv:1903.09471 [hep-lat].
- [24] J. Bijnens, N. Hermansson-Truedsson, and A. Rodríguez-Sánchez, Phys. Lett. **B798**, 134994 (2019), arXiv:1908.03331 [hep-ph].
- [25] G. Colangelo, F. Hagelstein, M. Hoferichter, L. Laub, and P. Stoffer, Phys. Rev. **D101**, 051501 (2020), arXiv:1910.11881 [hep-ph].
- [26] G. Colangelo, F. Hagelstein, M. Hoferichter, L. Laub, and P. Stoffer, JHEP **03**, 101 (2020), arXiv:1910.13432 [hep-ph].
- [27] T. Blum, N. Christ, M. Hayakawa, T. Izubuchi, L. Jin, C. Jung, and C. Lehner, Phys. Rev. Lett. **124**, 132002 (2020), arXiv:1911.08123 [hep-lat].
- [28] G. Colangelo, M. Hoferichter, A. Nyffeler, M. Passera, and P. Stoffer, Phys. Lett. **B735**, 90 (2014), arXiv:1403.7512 [hep-ph].
- [29] G. W. Bennett *et al.* (Muon $g - 2$), Phys. Rev. **D73**, 072003 (2006), arXiv:hep-ex/0602035 [hep-ex].
- [30] B. Chakraborty *et al.* (Fermilab Lattice, LATTICE-HPQCD, MILC), Phys. Rev. Lett. **120**, 152001 (2018), arXiv:1710.11212 [hep-lat].
- [31] S. Borsanyi *et al.* (Budapest-Marseille-Wuppertal), Phys. Rev. Lett. **121**, 022002 (2018), arXiv:1711.04980 [hep-lat].
- [32] T. Blum, P. A. Boyle, V. Gülpers, T. Izubuchi, L. Jin, C. Jung, A. Jüttner, C. Lehner, A. Portelli, and J. T. Tsang (RBC, UKQCD), Phys. Rev. Lett. **121**, 022003 (2018), arXiv:1801.07224 [hep-lat].
- [33] D. Giusti, V. Lubicz, G. Martinelli, F. Sanfilippo, and S. Simula (ETM), Phys. Rev. **D99**, 114502 (2019), arXiv:1901.10462 [hep-lat].
- [34] E. Shintani and Y. Kuramashi, Phys. Rev. **D100**, 034517 (2019), arXiv:1902.00885 [hep-lat].
- [35] C. T. H. Davies *et al.* (Fermilab Lattice, LATTICE-HPQCD, MILC), Phys. Rev. **D101**, 034512 (2020), arXiv:1902.04223 [hep-lat].
- [36] A. Gérardin, M. Cè, G. von Hippel, B. Hörz, H. B. Meyer, D. Mohler, K. Ottnad, J. Wilhelm, and H. Wittig, Phys. Rev. **D100**, 014510 (2019), arXiv:1904.03120 [hep-lat].
- [37] C. Aubin, T. Blum, C. Tu, M. Golterman, C. Jung, and S. Peris, Phys. Rev. **D101**, 014503 (2020), arXiv:1905.09307 [hep-lat].
- [38] D. Giusti and S. Simula, PoS **LATTICE2019**, 104 (2019), arXiv:1910.03874 [hep-lat].
- [39] S. Borsanyi *et al.*, (2020), arXiv:2002.12347 [hep-lat].
- [40] V. Pauk and M. Vanderhaeghen, Eur. Phys. J. **C74**, 3008 (2014), arXiv:1401.0832 [hep-ph].
- [41] I. Danilkin and M. Vanderhaeghen, Phys. Rev. **D95**, 014019 (2017), arXiv:1611.04646 [hep-ph].
- [42] F. Jegerlehner, Springer Tracts Mod. Phys. **274**, 1 (2017).
- [43] M. Knecht, S. Narison, A. Rabemananjara, and D. Rabetiariyony, Phys. Lett. **B787**, 111 (2018), arXiv:1808.03848 [hep-ph].
- [44] G. Eichmann, C. S. Fischer, and R. Williams, Phys. Rev. **D101**, 054015 (2020), arXiv:1910.06795 [hep-ph].
- [45] P. Roig and P. Sánchez-Puertas, Phys. Rev. **D101**, 074019 (2020), arXiv:1910.02881 [hep-ph].
- [46] M. Passera, W. Marciano, and A. Sirlin, Phys. Rev. **D78**, 013009 (2008), arXiv:0804.1142 [hep-ph].
- [47] A. Crivellin, M. Hoferichter, C. A. Manzari, and M. Montull, Phys. Rev. Lett. **125**, 091801 (2020), arXiv:2003.04886 [hep-ph].
- [48] A. Keshavarzi, W. J. Marciano, M. Passera, and A. Sirlin, Phys. Rev. **D102**, 033002 (2020), arXiv:2006.12666 [hep-ph].
- [49] B. Malaescu and M. Schott, (2020), arXiv:2008.08107 [hep-ph].
- [50] S. M. Roy, Phys. Lett. **36B**, 353 (1971).
- [51] B. Ananthanarayan, G. Colangelo, J. Gasser, and H. Leutwyler, Phys. Rept. **353**, 207 (2001), arXiv:hep-ph/0005297 [hep-ph].
- [52] R. García-Martín, R. Kamiński, J. R. Peláez, J. Ruiz de Elvira, and F. J. Ynduráin, Phys. Rev. **D83**, 074004 (2011), arXiv:1102.2183 [hep-ph].
- [53] I. Caprini, G. Colangelo, and H. Leutwyler, Eur. Phys. J. **C72**, 1860 (2012), arXiv:1111.7160 [hep-ph].
- [54] C. Bouchiat and L. Michel, J. Phys. Radium **22**, 121 (1961).
- [55] S. J. Brodsky and E. de Rafael, Phys. Rev. **168**, 1620 (1968).
- [56] R. Omnès, Nuovo Cim. **8**, 316 (1958).
- [57] J. F. de Trocóniz and F. J. Ynduráin, Phys. Rev. **D65**, 093001 (2002), arXiv:hep-ph/0106025 [hep-ph].
- [58] H. Leutwyler, Continuous advances in QCD **2002**, 23 (2002), arXiv:hep-ph/0212324 [hep-ph].
- [59] G. Colangelo, Nucl. Phys. Proc. Suppl. **131**, 185 (2004), arXiv:hep-ph/0312017 [hep-ph].
- [60] J. F. de Trocóniz and F. J. Ynduráin, Phys. Rev. **D71**, 073008 (2005), arXiv:hep-ph/0402285 [hep-ph].
- [61] M. Hoferichter, B. Kubis, J. Ruiz de Elvira, H.-W. Hammer, and U.-G. Meißner, Eur. Phys. J. **A52**, 331 (2016), arXiv:1609.06722 [hep-ph].
- [62] C. Hanhart, S. Holz, B. Kubis, A. Kupść, A. Wirzba, and C. W. Xiao, Eur. Phys. J. **C77**, 98 (2017), [Erratum: Eur. Phys. J. **C78**, 450 (2018)], arXiv:1611.09359 [hep-ph].

- [63] B. Ananthanarayan, I. Caprini, and D. Das, Phys. Rev. **D98**, 114015 (2018), arXiv:1810.09265 [hep-ph].
- [64] B. Ananthanarayan, I. Caprini, and D. Das, Phys. Rev. D **102**, 096003 (2020), arXiv:2008.00669 [hep-ph].
- [65] J. Batley *et al.* (NA48/2), Eur. Phys. J. **C70**, 635 (2010).
- [66] J. Batley *et al.* (NA48/2), Phys. Lett. **B715**, 105 (2012), [Addendum: Phys. Lett. **B740**, 364 (2015)], arXiv:1206.7065 [hep-ex].
- [67] G. Colangelo, E. Passemar, and P. Stoffer, Eur. Phys. J. **C75**, 172 (2015), arXiv:1501.05627 [hep-ph].
- [68] B. Hyams *et al.*, Nucl. Phys. **B64**, 134 (1973).
- [69] S. Protopopescu *et al.*, Phys. Rev. **D7**, 1279 (1973).
- [70] K. M. Watson, Phys. Rev. **95**, 228 (1954).
- [71] L. Łukaszyk, Phys. Lett. **47B**, 51 (1973).
- [72] S. Eidelman and L. Łukaszyk, Phys. Lett. **B582**, 27 (2004), arXiv:hep-ph/0311366 [hep-ph].
- [73] S. R. Amendolia *et al.* (NA7), Nucl. Phys. **B277**, 168 (1986).
- [74] R. R. Akhmetshin *et al.* (CMD-2), Phys. Lett. **B527**, 161 (2002), arXiv:hep-ex/0112031 [hep-ex].
- [75] R. R. Akhmetshin *et al.* (CMD-2), Phys. Lett. **B578**, 285 (2004), arXiv:hep-ex/0308008 [hep-ex].
- [76] M. N. Achasov *et al.*, J. Exp. Theor. Phys. **101**, 1053 (2005), [Zh. Eksp. Teor. Fiz. **128**, 1201 (2005)], arXiv:hep-ex/0506076 [hep-ex].
- [77] M. N. Achasov *et al.*, J. Exp. Theor. Phys. **103**, 380 (2006), [Zh. Eksp. Teor. Fiz. **130**, 437 (2006)], arXiv:hep-ex/0605013 [hep-ex].
- [78] R. R. Akhmetshin *et al.*, JETP Lett. **84**, 413 (2006), [Zh. Eksp. Teor. Fiz. **84**, 491 (2006)], arXiv:hep-ex/0610016 [hep-ex].
- [79] R. R. Akhmetshin *et al.* (CMD-2), Phys. Lett. **B648**, 28 (2007), arXiv:hep-ex/0610021 [hep-ex].
- [80] F. Ambrosino *et al.* (KLOE), Phys. Lett. **B670**, 285 (2009), arXiv:0809.3950 [hep-ex].
- [81] B. Aubert *et al.* (BaBar), Phys. Rev. Lett. **103**, 231801 (2009), arXiv:0908.3589 [hep-ex].
- [82] F. Ambrosino *et al.* (KLOE), Phys. Lett. **B700**, 102 (2011), arXiv:1006.5313 [hep-ex].
- [83] J. P. Lees *et al.* (BaBar), Phys. Rev. **D86**, 032013 (2012), arXiv:1205.2228 [hep-ex].
- [84] D. Babusci *et al.* (KLOE), Phys. Lett. **B720**, 336 (2013), arXiv:1212.4524 [hep-ex].
- [85] A. Anastasi *et al.* (KLOE-2), JHEP **03**, 173 (2018), arXiv:1711.03085 [hep-ex].
- [86] X. Feng, Y. Fu, and L.-C. Jin, Phys. Rev. **D101**, 051502 (2020), arXiv:1911.04064 [hep-lat].
- [87] G. Wang, J. Liang, T. Draper, K.-F. Liu, and Y.-B. Yang, (2020), arXiv:2006.05431 [hep-ph].
- [88] E. de Rafael, Phys. Rev. **D102**, 056025 (2020), arXiv:2006.13880 [hep-ph].
- [89] T. Horn *et al.* (Jefferson Lab F_π), Phys. Rev. Lett. **97**, 192001 (2006), arXiv:nucl-ex/0607005 [nucl-ex].
- [90] V. Tadevosyan *et al.* (Jefferson Lab F_π), Phys. Rev. **C75**, 055205 (2007), arXiv:nucl-ex/0607007 [nucl-ex].
- [91] G. M. Huber *et al.* (Jefferson Lab F_π), Phys. Rev. **C78**, 045203 (2008), arXiv:0809.3052 [nucl-ex].
- [92] H. P. Blok *et al.* (Jefferson Lab F_π), Phys. Rev. **C78**, 045202 (2008), arXiv:0809.3161 [nucl-ex].
- [93] D. J. Wilson, R. A. Briceño, J. J. Dudek, R. G. Edwards, and C. E. Thomas, Phys. Rev. **D92**, 094502 (2015), arXiv:1507.02599 [hep-ph].
- [94] G. S. Bali, S. Collins, A. Cox, G. Donald, M. Göckeler, C. Lang, and A. Schäfer (RQCD), Phys. Rev. **D93**, 054509 (2016), arXiv:1512.08678 [hep-lat].
- [95] D. Guo, A. Alexandru, R. Molina, and M. Döring, Phys. Rev. **D94**, 034501 (2016), arXiv:1605.03993 [hep-lat].
- [96] Z. Fu and L. Wang, Phys. Rev. **D94**, 034505 (2016), arXiv:1608.07478 [hep-lat].
- [97] C. Alexandrou, L. Leskovec, S. Meinel, J. Negele, S. Paul, M. Petschlies, A. Pochinsky, G. Rendon, and S. Syritsyn, Phys. Rev. **D96**, 034525 (2017), arXiv:1704.05439 [hep-lat].
- [98] C. Andersen, J. Bulava, B. Hörz, and C. Morningstar, Nucl. Phys. **B939**, 145 (2019), arXiv:1808.05007 [hep-lat].
- [99] M. Werner *et al.* (Extended Twisted Mass), Eur. Phys. J. **A56**, 61 (2020), arXiv:1907.01237 [hep-lat].
- [100] F. Erben, J. R. Green, D. Mohler, and H. Wittig, Phys. Rev. **D101**, 054504 (2020), arXiv:1910.01083 [hep-lat].
- [101] M. Fischer, B. Kostrzewa, M. Mai, M. Petschlies, F. Pittler, M. Ueding, C. Urbach, and M. Werner (ETM), (2020), arXiv:2006.13805 [hep-lat].
- [102] M. Niehus, M. Hoferichter, B. Kubis, and J. Ruiz de Elvira, (2020), arXiv:2009.04479 [hep-ph].
- [103] V. Aul'chenko *et al.* (CMD-2), JETP Lett. **82**, 743 (2005), arXiv:hep-ex/0603021.
- [104] M. Fujikawa *et al.* (Belle), Phys. Rev. **D78**, 072006 (2008), arXiv:0805.3773 [hep-ex].
- [105] M. Ablikim *et al.* (BESIII), Phys. Lett. **B753**, 629 (2016), arXiv:1507.08188 [hep-ex].
- [106] M. Ablikim *et al.* (BESIII), (2020), arXiv:2009.05011 [hep-ex].
- [107] M. Achasov *et al.* (SND), (2020), arXiv:2004.00263 [hep-ex].
- [108] F. Ignatov *et al.* (CMD-3), EPJ Web Conf. **212**, 04001 (2019).
- [109] G. Abbiendi *et al.*, Eur. Phys. J. **C77**, 139 (2017), arXiv:1609.08987 [hep-ex].
- [110] P. Banerjee *et al.*, Eur. Phys. J. **C80**, 591 (2020), arXiv:2004.13663 [hep-ph].